ARTICLE

Supplementary information on: A novel process towards the industrial realization of large-scale oxymethylene dimethyl ether production - COMET

Franz Mantei, Christian Schwarz, Ali Elwalily, Florian Fuchs, Andrew Pounder, Hendrik Stein, Matthias Kraume and Ouda Salem

1. Extended description of various OME processes

1.1. OME_1 and TRI (anhydrous synthesis)

Schelling et al.[1] proposed a process concept for the anhydrous synthesis and purification of OME_{3-5} from OME_1 and TRI, which was updated by Burger et al.[2,3] reducing the number of distillation columns to two. The feed mixture of OME_1 and TRI is mixed with the recycle streams and synthesized in the reactor as shown in Figure 1 in the manuscript. The OME synthesis proceeds fast, as shown in Figure S1 (a), which presents the experimental result of the OME synthesis from OME_1 and TRI by Burger[2]. Furthermore, a comparatively high selectivity for OME_{3-5} is obtained with very low side product formations using the catalyst Amberlyst® 46 (A46), as shown in Figure S1 (b). The choice of catalyst is crucial for the reaction kinetics and side product formation. Using A36, Burger detected the side products MEFO and DME, while only traces of MEFO could be detected with A46 at temperatures higher than 75 °C. Mantei et al.[4] also investigated the OME synthesis from OME_1 and TRI over various catalysts and reported comparatively high side product formations for zeolites but low side product formations for A46, Dowex and Nafion at 60 °C.

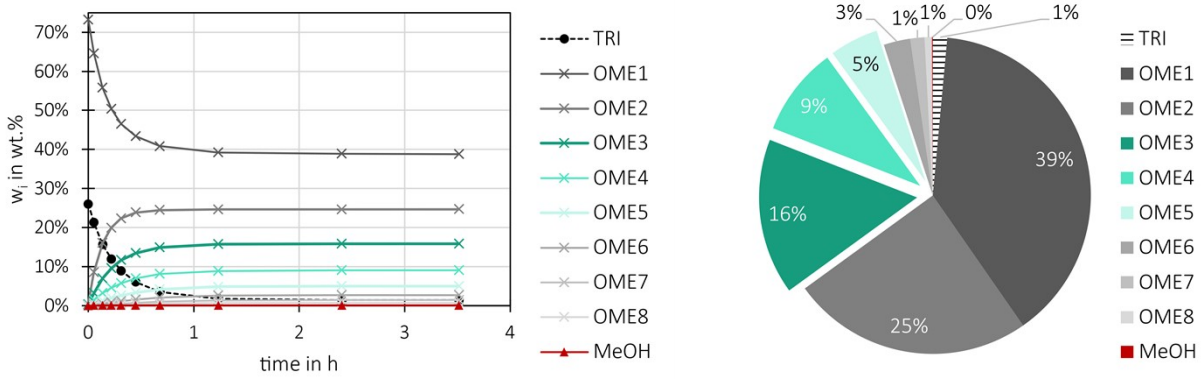

Figure S1 – OME synthesis from OME_1 and TRI over A46 (conditions: OME_1/TRI = 2.85 g/g, A46/(OME_1+TRI) = 0.8 wt%, 65 °C, batch) by Burger[3]. (a) shows the reaction progress and (b) shows the equilibrium composition. The values describe the mass fractions of the synthesis products.

After the reactor, the synthesis product mainly containing OME_{1-10}, FA and TRI is separated in a first distillation column to separate $OME_{\geq 3}$ from the more volatile components OME_{1-2}, FA and TRI. The distillate product is recycled to the reactor and the bottom product is separated in a second distillation column to provide the target product containing OME_{3-5} which is separated from the process and a bottom product containing $OME_{\geq 6}$ which are recycled to the reactor.

The advantages of this process concept are the simple design and no formation and, therefore, necessary separation of H_2O from the loop. However, Lautenschütz[5] investigated in a blank experiment the conversion of OME_1 alone in presence of the catalyst A36. Besides OME_1, the product mixture contained 2 wt% MeOH and 3 wt% OME_2. In a subsequent experiment he dried OME_1 before the addition of A36 and no MeOH or OME_2 could be detected in the product mixture. This emphasizes the need for a very dry feedstock to prevent the formation and finally accumulation of H_2O inside the process loop.

The main disadvantage of this process concept is the preparation of the feedstock TRI which is complex and energy-intensive, mainly due to the low conversion of FA to TRI in the reactor and the resulting high recycle streams.[6–9]

In comparison to alternative process routes the conversion of OME_1 and TRI to OME_{3-5} shows the advantage of a high OME_{3-5} yield which leads to an increase of the mass fraction of OME_{3-5} from 5 to 34 wt% before and after the reactor.[7] Therefore, comparatively

small recycle rates are obtained in the loop and the two distillation columns for the product purification require a low heat demand of about 8 % in comparison to the energy content of the OME_{3-5} product based on the lower heating value (LHV), as presented in Table 8 in the manuscript.[7] However, this advantage is outweighed by the energy-intensive feedstock preparation, resulting in an overall energy efficiency of 29-37 % considering the entire process chain from H_2O electrolysis and CO_2 capture via the MeOH, FA, TRI and OME_1 production towards the final OME_{3-5} product mixture.[7]
Considering the possibility of scale-up for a sustainable OME_{3-5} production based on OME_1 and TRI, the sub-processes for the production of MeOH (from CO_2 and H_2), FA, TRI and OME_1 are state-of-the-art and, therefore, show high technology readiness level (TRL).[10–12] Furthermore, the sub-process of the OME_{3-5} production only consists of state-of-the-art process units. Therefore, this process is an energy-intensive but feasible process concept for the production of OME_{3-5} in the near future.

1.2. DME and TRI (anhydrous synthesis)

Ströfer et al.[13,14] proposed a process concept for the anhydrous synthesis and purification of OME_{3-5} from DME and TRI similar to the process concept for OME_1 and TRI, as illustrated in Figure 1 in the manuscript. Due to the high vapor pressure of DME, the synthesis and first distillation column are operated at elevated pressure levels, which leads to a far higher reboiler temperature of about 300 °C in comparison to alternative processes with temperatures around 200 °C. This results in more expensive heat sources. Furthermore, the stability regarding thermal decomposition of OME should be experimentally investigated at this high temperature level. The main advantage of this process concept is the absence of H_2O. Furthermore, DME is a cheaper feedstock than OME_1.[15] However, the main disadvantage is the complex and energy-intensive preparation of TRI.[6–9]
Considering the experimental results of Haltenort et al.[16,17], Drexler et al.[18,19] and Breitkreuz et al.[20] regarding the OME synthesis from DME and TRI, the synthesis proceeds slow, as shown in Figure S2 (a). Furthermore, a lower yield of OME_{3-5} is obtained with very high side product formations for various catalyst systems and already at comparatively low temperatures of 80 °C, as shown in Figure S2 (b).[18,20] The highest OME_{3-5} concentration was obtained after 76 h, whereas the mixture still contained a high share of unreacted feedstock. For longer retention times, the concentration of OME_{3-5} reduced, due to an increasing formation of MEFO and FOAC. Unfortunately, the catalyst A46, which shows very small side product formations in the OME synthesis from OME_1 and TRI, is not active for this feedstock, due to its low acid concentration.[20]

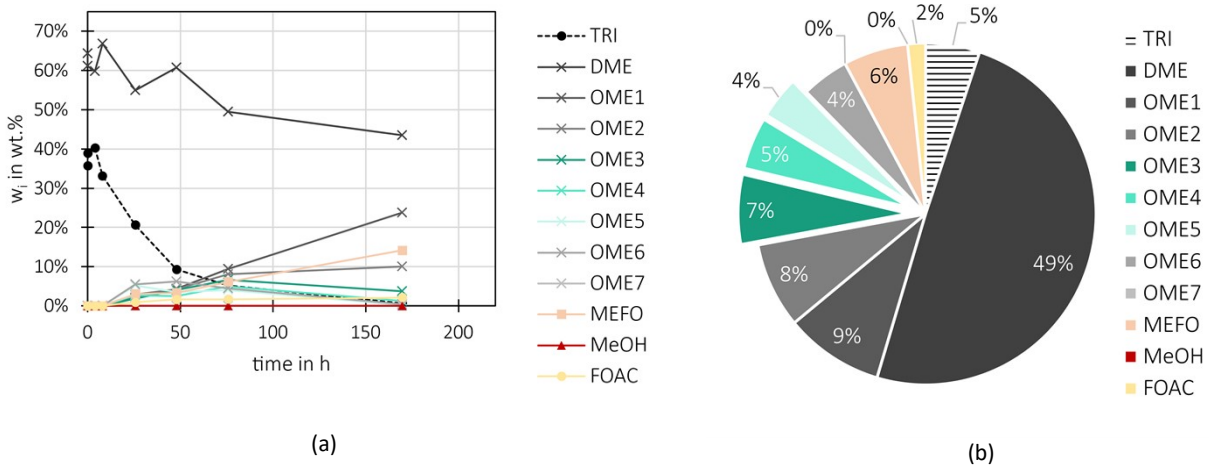

Figure S2 – OME synthesis from DME and TRI over A36 (conditions: DME/TRI = 1.80 g/g, A36/(DME+TRI) = 4.4 wt.%, 90 °C, batch) by Breitkreuz et al.[20]. (a) shows the reaction progress and (b) shows the composition after 76 h with the highest concentration of OME_{3-5}. The values describe the mass fractions of the synthesis products.

Besides OME, especially MEFO is produced with an increasing yield. For long retention times the yield of MEFO exceeds the yield of the product OME_{3-5}. Therefore, the process concept needs to be adjusted to include the separation and purification of MEFO as a valuable side product. However, due to the narrow boiling point between OME_1 and MEFO a high purity separation using distillation columns is challenging.[21,22] This also complicates a sustainable production of OME_{3-5} based on DME and TRI in the near future.

1.3. DME and monomeric FA (anhydrous synthesis)

To date there is no process concept published for the OME production from DME and monomeric FA. However, this process was investigated in the frame of the NAMOSYN project in which different OME_{3-5} production processes were evaluated and compared.[12,23] The process concept for the production of OME_{3-5} from DME and monomeric FA is similar to the process from OME_1 and TRI, as illustrated in Figure 1 in the manuscript. Furthermore, the same advantage of an anhydrous synthesis can be obtained, which potentially leads to comparatively high OME_{3-5} yields. The feedstock DME is cheaper than OME_1 and the production of monomeric FA shows potential to become simpler and cheaper than the production of TRI. In comparison to the partial oxidation

of MeOH, as described in eqn (15) in the manuscript, the dehydrogenation of MeOH towards FA produces H_2 instead of H_2O as a by-product.[24] H_2 can be separated and recycled to the MeOH synthesis, which results in a stochiometrically lower H_2 demand and potentially reduces the production costs, since the feedstock H_2 generally has the biggest share on the production costs for various PtX products, considering a sustainable production.[12,15] Moreover, using monomeric FA instead of TRI might reduce the formation of side products in comparison to the OME synthesis based on DME and TRI. However, the main disadvantages are a very low TRL of the anhydrous FA synthesis and many open investigations regarding its usage for the synthesis of OME.[12] So far, the anhydrous FA synthesis was investigated in laboratory experiments.[24,25] Investigations regarding catalyst deactivation and long-term experimeriments are still to be successfully completed before its demonstration. Furthermore, besides the synthesis, the monomeric FA product is gaseous and needs to be absorbed from the synthesis product mixture without using H_2O or MeOH as a washing liquid, which are used for the FA(aq.) separation but would lead to the formation of many side products in the OME synthesis, as described by eqn (1)-(4) in the manuscript. The washing liquid should either be DME, the recycle stream containing the volatile components in the OME_{3-5} sub-process, or a separate component which does not react in the OME synthesis and can be separated and recycled to the absorption column. The solubility of monomeric FA in DME, OME or other suitable candidates should be investigated at suitable conditions for the absorption, which strongly differs between the washing liquids, to provide a liquid product stream. Therefore, a demonstration and scale-up for a sustainable production of OME_{3-5} based on DME and monomeric FA is unlikely in the near future.

1.4. OME_1 and monomeric FA (anhydrous route)

Mantei et al.[12] proposed a process concept for the anhydrous synthesis and purification of OME_{3-5} from OME_1 and monomeric FA, similar to the process concept for OME_1 and TRI, as illustrated in Figure 1 in the manuscript. They included a H_2O separation unit for the distillate product of the first distillation column to separate traces of H_2O, which entered the process from the OME_1 feedstock. This unit can also be omitted if a high purity OME_1 feedstock can be provided. In comparison to the feedstock DME, OME_1 is more expensive.[15] However, synthesis experiments with similar feedstocks of OME_1 and TRI and OME_1 and pFA show comparatively high selectivities and low side product formations, if the temperature is kept below 80 °C and a suitable catalyst system is used.[2,26] Peter et al.[27] investigated the synthesis of OME_1 and gaseous monomeric FA and found a comparatively high selectivity towards OME_{3-5} with low side product formations of MEFO and TRI, see Figure S3. With a smaller ratio of OME_1 to FA the yield of OME_{3-5} can be further increased.

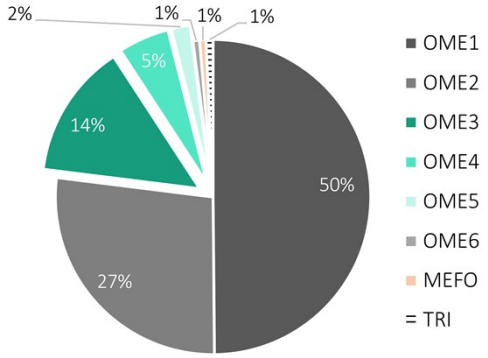

Figure S3 – OME synthesis from OME_1 and monomeric FA over $OMe_3^+BF_4^-$ in $EMIM^+BF_4^-$ (ionic liquid) (conditions: OME_1/FA = 1.58 g/g, $OMe_3^+BF_4^-/OME_1$ = 2-3 mol.%, 45 °C, continuous addition of gaseous FA) by Peter et al.[27]. The values describe the mass fractions of the synthesis product.

Besides the advantage of a potentially simpler and cheaper production of monomeric FA in comparison to TRI, similar challenges to the OME production based on DME and monomeric FA need to be investigated. The provision of the feedstock in the liquid phase and the demonstration of the anhydrous FA synthesis. Mantei et al.[12] assumed that the recycle stream of the volatile components from the OME_{3-5} sub-process is used to absorb monomeric FA from the FA synthesis mixture. However, they pointed out that the absorption of monomeric FA is a crucial process step, and the assumption of a good solubility should be experimentally investigated. Peter et al.[27] observed that the addition of gaseous FA to OME_1 without the presence of a catalyst led to instant polymerization. This indicates a low solubility of monomeric FA in OME_1. Zimao et al.[28] on the other hand emphasized a good solubility of FA in OME_2.

Regarding the process performance, the conversion of OME_1 and monomeric FA shows the potential of a high OME_{3-5} yield which leads to an increase of the mass fraction of OME_{3-5} from 5 to 29 wt% before and after the reactor.[12] This leads to small recycle rates and results in a heat demand for the two distillation columns of about 11 % in comparison to the energy content of the final OME_{3-5} product based on the LHV. Considering the assumption from Held et al.[7] regarding H_2O electrolysis and CO_2 capture, results in an overall energy efficiency of 27-36%, including the production of the intermediate products MeOH, FA and OME_1.[12] However, due to the low TRL of the monomeric FA production a demonstration and scale-up of the sustainable production of OME_{3-5} based on OME_1 and monomeric FA is unlikely for the near future.

1.5. MeOH and FA(aq.) (aqueous synthesis)

Schmitz et al.[29,30] proposed a process concept for the aqueous synthesis and purification of OME_{3-5} from MeOH and concentrated aqueous FA solutions FA(aq.). The process concept is similar to the concept for OME_1 and TRI, with the addition of a H_2O separation unit, as illustrated in Figure 1 in the manuscript. The feed mixture of MeOH and concentrated FA(aq.) is mixed with the recycle streams and synthesized in the reactor. The OME synthesis proceeds fast, as shown in Figure S4 (a), which illustrates the experimental result of the OME synthesis from MeOH and pFA by Schmitz et al.[31]. However, due to the presence of H_2O and MeOH, FA reacts to HF and MG, as described by eqn (1)-(4) in the manuscript. Therefore, a comparatively low selectivity of OME_{3-5} is obtained, as shown in Figure S4 (b). This can be increased by adding more FA to MeOH, but the fraction of OME_{3-5} stays significantly smaller in comparison to the anhydrous routes. Using the catalyst A46, only traces of MEFO and TRI were detected.[32]

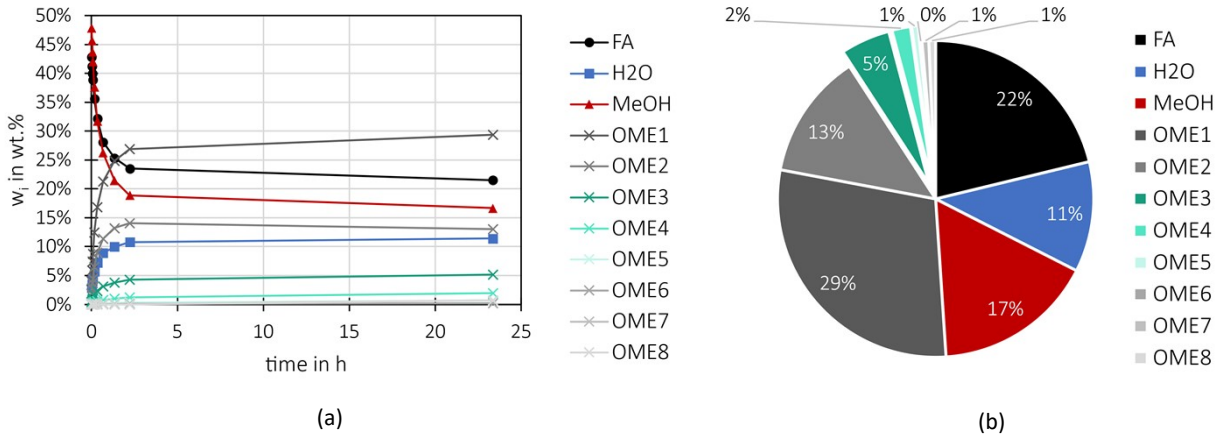

Figure S4 – OME synthesis from MeOH and pFA over A46 (conditions: FA/MeOH = 0.89 g/g, A46/(MeOH+pFA) = 1.9 wt.%, 60 °C, batch) by Schmitz et al.[31]. (a) shows the reaction progress and (b) shows the equilibrium composition. The values describe the mass fractions of the synthesis products.

After the reactor, the synthesis product mainly contains FA, H_2O, MeOH, HF, MG and OME_{1-10} and is separated in a first distillation column to separate $OME_{\geq 3}$ from the more volatile components FA, H_2O, MeOH, HF, MG and OME_{1-2}. The distillate product is sent to a H_2O separation unit and afterwards recycled to the reactor. The bottom product is separated into the target product OME_{3-5} which is separated from the process and $OME_{\geq 6}$ which are recycled back to the reactor. The main advantage of this process concept is the feedstock, whose preparation is simpler than the feedstock for the anhydrous routes. However, the main disadvantage is the formation of H_2O as a side product, which decreases the selectivity towards OME_{3-5} and needs to be separated from the loop. Schmitz et al.[29] proposed the utilization of adsorbents or a membrane to separate and extract the side product H_2O, which is described in detail in the manuscript.

In comparion to alternative process concepts, the conversion of MeOH and FA(aq.) to OME_{3-5} shows a low OME_{3-5} yield which leads to an increase of the mass fraction of OME_{3-5} from 0 to 15 wt% before and after the reactor.[7] Therefore, comparatively large recycle rates are obtained in the loop. The purification of the synthesis product is energy-intensive in the two distillation columns, whose reboiler duties sum up to about 47 % of the energy content of the OME_{3-5} product based on the LHV.[7] However, these disadvantages are outweighed by the comparatively simple feedstock preparation, resulting in an overall energy efficiency of 25-31%, considering the entire process chain from H_2O electrolysis and CO_2 capture, via the MeOH and FA production, towards the final OME_{3-5} product mixture.[12] The TRL of the production of the intermediate products MeOH and FA is very high and does not limit the scale-up of a sustainable OME_{3-5} production based on MeOH and FA. Recently a plant was built to demonstrate the production of OME_{3-5} from MeOH and FA covering all required process units and enabling the separation of H_2O using a membrane.[33,34] The membrane is the main bottleneck for a fast scale-up of this process concept, which, considering the application as a fuel, will easily grow above 100 kt/a OME_{3-5} for a single production plant, which results in about 24 kt/a H_2O to be separated from the distillate stream of about 520 kt/a.[12]

1.6. MeOH and monomeric FA (aqueous synthesis)

Mantei et al.[12] proposed a process concept for the aqueous synthesis and purification of OME_{3-5} from MeOH and monomeric FA, similar to the process concept from MeOH and concentrated FA(aq.), as illustrated in Figure 1 in the manuscript. The main advantages of this process concept are a simple preparation for the feedstock MeOH and a potentially simple preparation of the feedstock monomeric FA. The main disadvantages are the presence of H_2O in the OME synthesis and the low TRL of the monomeric FA production.

In comparison to the OME production based on MeOH and FA(aq.), the OME_{3-5} yield is slightly improved which leads to an increase of the mass fraction of OME_{3-5} from 3 to 19 wt% before and after the reactor.[12] This decreases the recycle rates. However, the purification of the synthesis product is still energy-intensive in the two distillation columns, with a heat demand of about 48 % of

the energy content of the OME_{3-5} product based on the LHV. Considering the entire process chain starting from H_2O electrolysis and CO_2 via the production of the indermediate products MeOH and FA towards the target product mixture OME_{3-5} and considering the assumptions from Held et al.[7] regarding the electricity and heat demand for the H_2O electrolysis and CO_2 preparation, an energy efficiency of 28-37% can be achieved. Due to the low TRL of the monomeric FA production and the necessity of a H_2O separation unit, a fast demonstration and scale-up of a sustainable production of OME_{3-5} based on MeOH and monomeric FA is unlikely in the near future.

1.7. OME_1 and FA(aq.) or pFA (aqueous synthesis)

Hackbarth et al.[35] published a list of OME production plants in China from which most of them are based on the feedstock OME_1 and pFA. The process concept is similar to the OME production process from OME_1 and TRI with the addition of a H_2O separation unit, as discussed by Mantei et al.[12]. Experimental results from Liu et al.[26] regarding the OME synthesis from OME_1 and pFA show that a comparatively high yield towards OME_{3-5} can be achieved, see Figure S5. This can still be increased by increasing the ratio of OME_1 to pFA.[26] However, they also reported that comparatively high temperatures of about 90 °C are beneficial for the depolymerization of pFA, which lead to a high formation of side products, i.e. MEFO and DME, using the catalyst NKC-9.

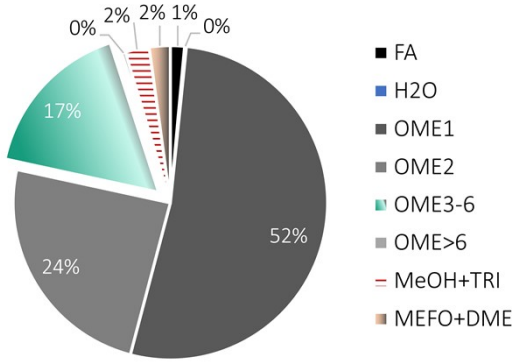

Figure S5 – OME synthesis from OME_1 and pFA over NKC-9 (conditions: OME_1/pFA = 4.31 g/g, NKC-9/(OME_1+pFA) = 5 wt.%, 3h, 90 °C, batch) by Liu et al.[26]. The values describe the mass fractions of the synthesis product.

The depolymerization of the solid pFA can be accelerated using concentrated FA(aq.) instead, which is an intermediate product for the pFA production and can be prepared using a cascade of evaporators, as discussed by Mantei et al.[12] and in the manuscript. The liquid concentrated FA(aq.) product mainly consist of MG which also need to depolymerize as described by eqn (4) in the manuscript, but from a smaller degree of polymerization. A disadvantage is the higher amount of H_2O in the feedstock, which reduces the selectivity towards OME_{3-5}.

The main advantage of the process concept is the comparatively high selectivity of OME_{3-5}, which is increasing with decreasing H_2O contents in the FA feedstock. Furthermore, production processes for the feedstocks are state-of-the-art. The main disadvantage is the presence of H_2O in the OME synthesis, which needs to be separated from the loop.

In comparison to the OME production from MeOH and FA(aq.) the selectivity of OME_{3-5} slightly increases, resulting in an increase of the mass fraction of OME_{3-5} from 4 to 19 wt% before and after the reactor.[12] This leads to a heat demand of about 26 % for the reboiler of the distillation columns in comparison to the energy content of the OME_{3-5} product based on the LHV. This is considerably lower than the heat demand for the OME production based on MeOH and FA(aq.). Considering the entire process chain starting from H_2O electrolysis and CO_2 via the production of the indermediate products MeOH, FA and OME_1 towards the target product mixture OME_{3-5} and considering the assumptions from Held et al.[7] regarding the electricity and heat demand for the H_2O electrolysis and CO_2 preparation, an energy efficiency of 26-32 % can be achieved. Similar to the production of OME_{3-5} from MeOH and FA(aq.), the H_2O separation unit is the bottleneck for the scale-up of this process concept.

1.8. Further process concepts for the production of OME_{3-5}

The processes described above for the production of OME_{3-5} are comparatively simple and efficient and contain the potential of a comparatively fast scale-up, after the main bottlenecks are overcome and the feasibility is successfully demonstrated. However, various process alternatives were published, which are more complex, contain unrealistic configuration or redundant feedstock combination.

An OME_{3-5} production in China is based on the feedstock MeOH and TRI, which has the disadvantage of the energy-intensive TRI production and still requires a H_2O separation unit inside the OME_{3-5} sub-process[5,35]. Therefore, the OME_{3-5} production based on OME_1 and TRI is simpler and it can already be scaled up.

Palkovits et al.[36,37] proposed a process concept for the production of OME_{3-5} based on MeOH or OME_1 and FA. For the separation of OME_{1-2} from H_2O and MeOH, OME_{1-2} are adsorbed on activated carbon or hypercrosslinked polymers. However, H_2O still needs to be separated from the loop, preferably from MeOH and FA, to obtain higher yields of OME_{3-5}.
Hagen et al.[38] proposed a process for the production of OME_{3-5} based on DME and FA. DME is used to produce FA and after the separation of DME, OME are formed and separated in a reactive distillation column. In the described configuration it is unlikely that $OME_{\geq 2}$ are formed and separated from the reactive distillation column in satisfying yields. Drunsel[39] investigated a similar feed mixture in a reactive distillation column to produce OME_1 without reporting the presence of $OME_{\geq 2}$.
Qiang et al.[40] proposed a process for the production of OME_{3-5} based on OME_1 and $OME_{\geq 6}$. The main advantages are an anhydrous synthesis without the need to separate H_2O, high yields of OME_{3-5} and, therefore, a simple product purification. However, the availability of the feedstock $OME_{\geq 6}$ is comparatively low since it is a by-product of the OME synthesis and there usually recycled back to the reactor.
Furthermore, OME_{3-5} production processes whose main bottleneck is the separation of H_2O from the loop can certainly already be constructed and scaled-up, if the operators accept and handle large by-product streams which still contain significant amounts of unreacted feedstock and OME_2. This can be attractive if other processes are available which can use this by-product stream as a feedstock, such as the process for the production of OME_1. However, the scale of the by-product streams would exceed the OME_{3-5} product stream, which would result is significantly lower yields of OME_{3-5}. Considering the application of OME_{3-5} in the mobility sector as a diesel fuel additive or alternative, many large-scale plants are needed, which would very soon exceed the demand for the products of the waste stream handling processes.

2. H_2O separation from the production of OME

2.1. Extraction

Figure S6 illustrates the results of Li et al.[41] regarding the separation of the OME synthesis product using toluene.

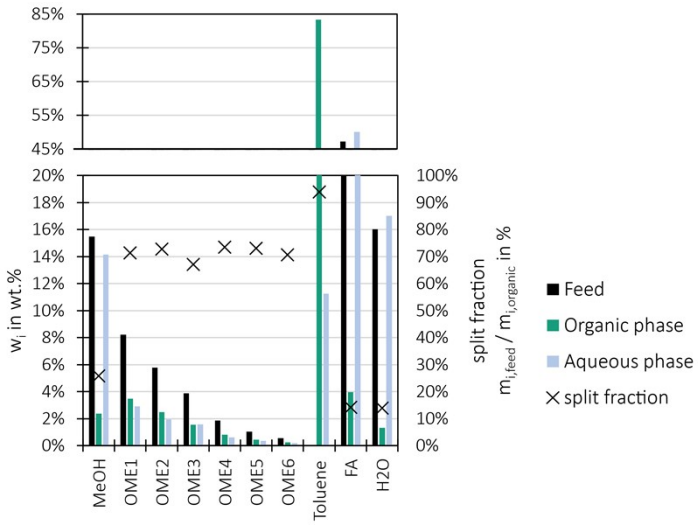

Figure S6 – H_2O separation from the OME synthesis product using toluene as extracting agent (conditions: (OME synthesis product)/toluene = 0.667 g/g, 25 °C, batch) by Li et al.[41]

In addition to the extraction method discussed in the manuskript, Oestreich et al.[42] investigated the extraction of OME from H_2O, MeOH, FA and TRI using hydrocarbons, i.e. n-dodecane, diesel and hydrogenated vegetable oil (HVO) as extracting agents. They proposed to use the hydrocarbons already during the synthesis to gain a product phase containing OME_n with hydrocarbons and an aqueous phase containing MeOH, FA, H_2O and the catalyst. For the application as a fuel OME_1 should be separated to increase the flash point which will also separate most of the H_2O content in the product phase. Their analysis showed that the remaining mixture of HVO or diesel fuel with about 7 wt% $OME_{2\text{-}10}$ complies to current fuel standards to a large extend.

2.2. Adsorption

Figure S7 illustrates the results of Schmitz et al.[29] regarding the adsorption of H_2O from a mixture containing FA, H_2O, MeOH and $OME_{1\text{-}4}$ using zeolite 3A.

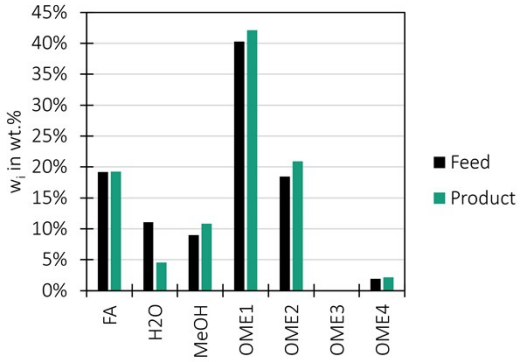

Figure S7 – H_2O separation from the OME synthesis product via adsorption using zeolite 3A (conditions: (OME mixture)/(zeolite 3A) = 2.0 g/g, 25 °C, batch) by Schmitz et al.[29]

2.3. Membrane

Figure S8 illustrates the results of Schmitz et al.[43] regarding the separation of H_2O from a mixture containing FA, H_2O, MeOH, OME_1 and OME_2 using the PERVAP 4100 membrane.

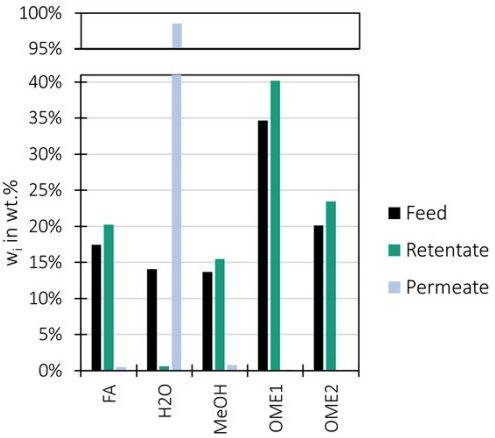

Figure S8 – H_2O separation from the OME synthesis product using the polymeric membrane PERVAP 4100 (conditions: 80 °C, 2 mbar permeate, 80 l/h) by Schmitz et al.[43]

3. Materials and Methods

3.1. Concentrated FA(aq.) feed preparation

A simplified process flow diagram of the feed preparation of the concentrated FA(aq.) solution is illustrated in Figure S9.

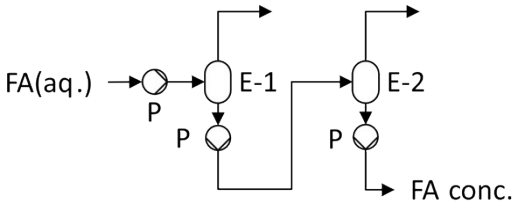

Figure S9 – Simplified process flow diagram for the concentration of an FA(aq.) to 85-88 wt% FA using a cascade of two evaporators operated at 200-600 mbar and 100-150 °C heating fluid. E, evaporator; P, pump.

3.2. OME synthesis

A simplified process flow diagram of the OME synthesis setup is illustrated in Figure S10.

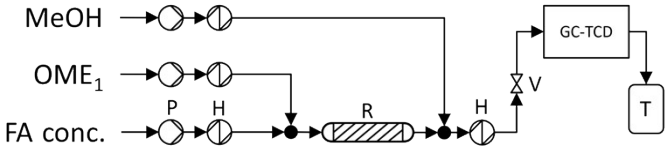

Figure S10 – Simplified process flow diagram for the OME synthesis of OME_1 and concentrated FA(aq.) solution over A46 for a capacity of 1-5 L/h at about 90 °C. H, heat exchanger; P, pump; R, reactor; T, tank; V, valve.

3.3. Thermal separation in CO-1

A simplified process flow diagram of the distillation setup is illustrated in Figure S11.

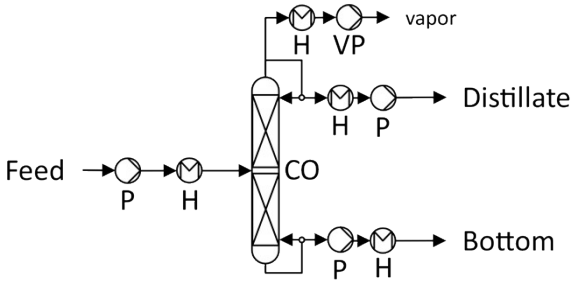

Figure S11 – Simplified process flow diagram of the DN 50 glas distillation setup for a feed rate of 1-5 L/h. CO, distillation column; H, heat exchanger; P, pump; VP, vacuum pump.

4. Results and Discussion

4.1. Experimental validation of the COMET process

4.1.1. OME synthesis

Fehler! Verweisquelle konnte nicht gefunden werden. lists the analytic results of the composition in the product barrels P1-P5. The concentrations are presented in mass fractions.

Table S1 – OME synthesis from OME_1 and concentrated FA(aq.) solution over A46 (conditions: concentrated FA(aq.) with 85-89 wt% FA, (concentrated FA(aq.) solution)/OME_1 = 0.6 g/g, A46/(OME_1+concentrated FA(aq.) solution) = 0.34 g/g h, approx. 3 L/h, 90 °C, 10 bar, fixed bed reactor). The concentrations are presented in mass fractions.

	P1-Exp	P2-Exp	P3-Exp	P4-Exp	P5-Exp
FA	0.2418	0.2434	0.1432	0.1526	0.1794
H_2O	0.0366	0.0394	0.0394	0.0394	0.0394
MeOH	0.1476	0.1557	0.0996	0.1083	0.1111
OME_1	0.3541	0.4141	0.2984	0.2808	0.2515
OME_2	0.1068	0.0673	0.2006	0.1926	0.1818
OME_3	0.0625	0.0413	0.1099	0.1116	0.1127
OME_4	0.0293	0.0212	0.0570	0.0597	0.0633
OME_5	0.0131	0.0104	0.0291	0.0309	0.0341
OME_6	0.0058	0.0050	0.0146	0.0156	0.0179
TRI	0.0014	0.0011	0.0065	0.0065	0.0068
Tetroxane	0.0003	0.0003	0.0008	0.0008	0.0009
MEFO	0.0007	0.0009	0.0009	0.0011	0.0011

4.1.2. Synthesis product separation in CO-1

Table S2 lists the analytic results of the composition of the distillate and bottom product mixture of CO-1. The concentrations are presented in mass fractions.

Table S2 – CO-1, OME synthesis product separation (conditions: 2 L/h, reflux/distillate = 0.5-2 s/s, distillate/feed = 81 wt%, Montz 750 structured packing, 85-175 °C, ambient pressure). The concentrations are presented in mass fractions.

	Distillate	Bottom
FA	0.1960	0.0006
H_2O	0.0471	0.0000
MeOH	0.1973	0.0000
OME_1	0.2725	0.0000
OME_2	0.2456	0.0000
OME_3	0.0176	0.4458
OME_4	0.0000	0.2645
OME_5	0.0000	0.1380
OME_6	0.0000	0.0714
TRI	0.0239	0.0000
Tetroxane	0.0001	0.0052
MEFO	0.0000	0.0000

4.1.3. Reactive distillation in CO-2

Table S3 lists the analytic results of the composition of the distillate and bottom product mixture of CO-2. The concentrations are presented in mass fractions.

Table S3 – CO-2, Reactive distillation of the distillate product of CO-1 over A46 (conditions: A46/(feed stream) = 0.35 g/g h, 1 L/h, distillate/feed = 63 wt% Montz 750 structured packing, 45-104 °C, ambient pressure). The concentrations are presented in mass fractions.

	Feed	Distillate	Bottom
FA	0.2047	0.0000	0.6100
H_2O	0.0486	0.0000	0.3800
MeOH	0.3031	0.0514	0.0035
OME_1	0.1984	0.9486	0.0006
OME_2	0.2202	0.0000	0.0001
OME_3	0.0158	0.0000	0.0004
OME_4	0.0000	0.0000	0.0005
OME_5	0.0000	0.0000	0.0003
OME_6	0.0000	0.0000	0.0002
TRI	0.0081	0.0000	0.0006
Tetroxane	0.0000	0.0000	0.0038
MEFO	0.0011	0.0000	0.0000

4.1.4. Product separation in CO-3

Table S4 lists the analytic results of the composition of the distillate and bottom product mixture of CO-3. The concentrations are presented in mass fractions.

Table S4 – CO-3, product separation (conditions: 5.5 L/h, distillate/feed = 82 wt%, Montz 750 structured packing, 100-210 °C, 200 mbar). The concentrations are presented in mass fractions.

	Feed	Distillate	Bottom
FA	0.0006	0.0013	0.0000
H_2O	0.0000	0.0001	0.0000
MeOH	0.0000	0.0003	0.0000
OME_1	0.0000	0.0001	0.0000
OME_2	0.0000	0.0002	0.0000
OME_3	0.4458	0.5184	0.0000
OME_4	0.2645	0.3402	0.0065
OME_5	0.1380	0.1296	0.2570
OME_6	0.0714	0.0021	0.3439
OME_7	0.0368	0.0001	0.1942
OME_8	0.0202	0.0000	0.1052
OME_9	0.0098	0.0000	0.0537
OME_{10}	0.0051	0.0000	0.0269
OME_{11}	0.0026	0.0000	0.0124
TRI	0.0000	0.0001	0.0000
Tetroxan	0.0052	0.0075	0.0000
MEFO	0.0000	0.0000	0.0000

4.2. Mass balance and operation conditions of the process units of the COMET process starting from H_2 and CO_2

4.2.1. MeOH sub-process

Figure S12 illustrates a simplified process flow diagram of the MeOH production based on H_2 and CO_2. Furthermore, it presents the stream numbering for the stream compositions and conditions listed in Table S5.

Table S5 – Stream table for the MeOH production based on H_2 and CO_2. The stream numbering is presented in Figure S12. The concentrations are presented in mass fractions.

	1	2	3	4	5	6	7	8	9	10	11	12	13	14	15	16	17	18	19
T in °C	59.5	25.0	240.1	250.1	40.0	47.7	40.0	62.0	60.0	131.9	47.7	60.0	60.0	84.1	58.2	58.2	58.2	59.9	99.5
p in bar	30.0	1.0	70.0	66.5	66.2	70.0	66.2	1.1	1.0	66.2	70.0	1.0	1.8	1.3	1.0	2.1	1.8	1.8	1.0
m in kg/h	3142	22674	95791	95796	66852	69975	28943	33302	8189	3830	707	25113	11171	13942	8917	5288	3616	14787	5025
H_2O	0.000	0.000	0.001	0.095	0.001	0.001	0.313	0.288	0.064	0.000	0.001	0.360	0.360	0.360	0.001	0.001	0.001	0.272	0.998
MeOH	0.000	0.000	0.006	0.174	0.009	0.008	0.555	0.592	0.450	0.007	0.008	0.639	0.639	0.639	0.998	0.999	0.999	0.727	0.002
H_2	1.000	0.000	0.147	0.115	0.165	0.156	0.000	0.000	0.001	0.003	0.156	0.000	0.000	0.000	0.000	0.000	0.000	0.000	0.000

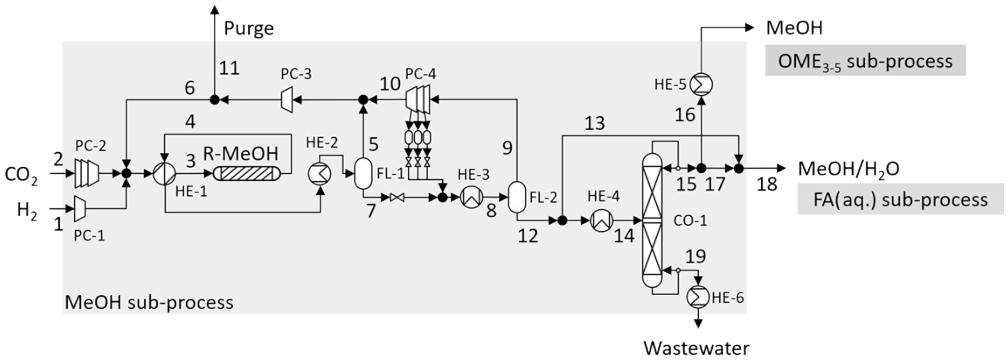

Figure S12 – Simplified process diagram for the production of MeOH from H_2 and CO_2. CO, distillation column; FL, phase separator; HE, heat exchanger; PC, compressor; R, reactor.

CO_2	0.000	1.000	0.800	0.569	0.760	0.771	0.130	0.118	0.478	0.976	0.771	0.001	0.001	0.001	0.002	0.000	0.000	0.001	0.000
CO	0.000	0.000	0.046	0.047	0.066	0.063	0.002	0.002	0.006	0.014	0.063	0.000	0.000	0.000	0.000	0.000	0.000	0.000	0.000

Table S6 to Table S10 present the operation conditions of the main process units of the MeOH sub-process including heat exchangers, a distillation column, reactor, phase separators and compressors.

Table S6 – Operation conditions of the heat exchangers used for the MeOH production based on H_2 and CO_2. Numbering is presented in Figure S12.

	HE-1	HE-2	HE-3	HE-4	HE-5	HE-6
Heat/cooling demand in MW	13.03	-13.52	2.14	3.21	1.69	-0.46
m in kg/h	95791	95796	33302	13942	5288	5025
$T_{1,in}$ in °C	74.7	130.1	34.4	59.9	58.2	99.5
$T_{1,out}$ in °C	240.1	40.0	62.0	84.1	81.0	30.0
$T_{2,in}$ in °C	250.1	-	-	-	-	-
$T_{2,out}$ in °C	130.1	-	-	-	-	-
p_1 in bar	70	66	1	1	2	1
p_2 in bar	66	-	-	-	-	-
$phase_{1,in}$	gas	gas/liquid	gas/liquid	liquid	liquid	liquid
$phase_{1,out}$	gas	gas/liquid	gas/liquid	gas/liquid	gas	liquid
$phase_{2,in}$	gas	-	-	-	-	-
$phase_{2,out}$	gas/liquid	-	-	-	-	-

Table S7 – Operation conditions of the distillation column used for the MeOH production based on H_2 and CO_2. Numbering is presented in Figure S12.

	CO-1
Heat demand in MW	4.03
Cooling demand in MW	-6.96
m_{Feed} in kg/h	13942
p in bar	1
T_{Dist} in °C	58.2
D:F in g/g	0.64
T_{Bott} in °C	99.5
number of stages	28
reflux:distillate in g/g	1.5

Table S8 – Operation conditions of the reactor used for the MeOH production based on H_2 and CO_2. Numbering is presented in Figure S12.

	R-MeOH
Cooling demand in MW	-7.35
m_{Feed} in kg/h	95791
T_{in} in °C	240
T_{out} in °C	250
p in bar	70
Reactor type	fixed bed reactor
Heat management	isothermal
$m_{Catalyst}$ in kg	84112
GHSV in h^{-1}	2639

Table S9 – Operation conditions of the phase separators used for the MeOH production based on H_2 and CO_2. Numbering is presented in Figure S12.

	FL-1	FL-2
Heat demand in MW	0.00	0.00
m_{Feed} in kg/h	95796	33302
p in bar	66	1
T in °C	40.0	62.0

Table S10 – Operation conditions of the compressors used for the MeOH production based on H_2 and CO_2. Numbering is presented in Figure S12.

	PC-1	PC-2	PC-3	PC-4
Power in MW	1.43	2.27	0.36	0.58
Cooling demand in MW	0.00	-1.67	0.00	-2.09
m_{Feed} in kg/h	3142	22674	70682	8189
p_{in} in bar	30	1	66	1
p_{out} in bar	70	70	70	66
T_{in} in °C	59.5	25.0	41.6	60.0
T_{out} in °C	173.1	132.1	47.7	131.9
$T_{intercooling}$ in °C	-	35	-	35
number of stages	1	4	1	4

4.2.2. FA(aq.) sub-process

Figure S13 illustrates a simplified process flow diagram of the FA(aq.) production based on MeOH and air. Furthermore, it presents the stream numbering for the stream compositions and conditions listed in Table S11.

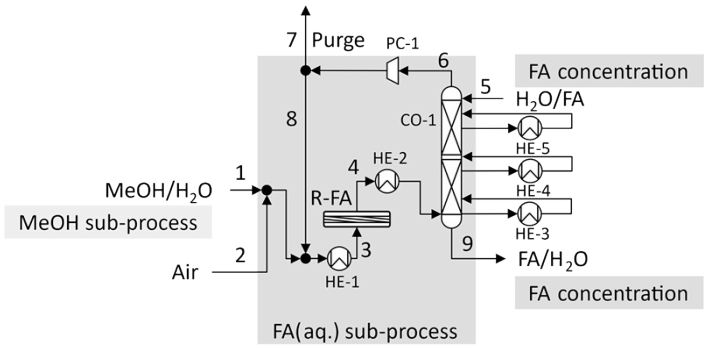

Figure S13 – Simplified process diagram for the production of FA(aq.) from MeOH and air. CO, distillation column; HE, heat exchanger; PC, compressor; R, reactor.

Table S11 – Stream table for the FA(aq.) production from MeOH and air. The stream numbering is presented in Figure S13. The concentrations are presented in mass fractions.

	1	2	3	4	5	6	7	8	9
T in °C	59.9	25.0	140.0	578.2	30.1	33.5	100.3	100.3	64.9
p in bar	1.8	1.8	1.4	1.3	1.0	1.0	1.8	1.8	1.0
m in kg/h	14787	21881	64566	64566	1231	47287	19388	27899	18509
FA	0.000	0.000	0.001	0.142	0.184	0.003	0.003	0.003	0.501
H_2O	0.272	0.000	0.077	0.150	0.795	0.033	0.033	0.033	0.491
MeOH	0.727	0.000	0.168	0.004	0.020	0.003	0.003	0.003	0.007
H_2	0.000	0.000	0.004	0.007	0.000	0.010	0.010	0.010	0.000
CO_2	0.001	0.000	0.025	0.042	0.000	0.058	0.058	0.058	0.000
CO	0.000	0.000	0.001	0.002	0.000	0.002	0.002	0.002	0.000
N_2	0.000	0.710	0.587	0.587	0.001	0.801	0.801	0.801	0.000
O_2	0.000	0.290	0.137	0.066	0.000	0.090	0.090	0.090	0.000

Table S12 to Table S15 present the operation conditions of the main process units of the FA(aq.) sub-process including heat exchangers, an absorber column, reactor and compressor.

Table S12 – Operation conditions of the heat exchangers used for the FA(aq.) production based on MeOH and air. Numbering is presented in Figure S13.

	HE-1	HE-2	HE-3	HE-4	HE-5
Heat/cooling demand in MW	7.59	-10.56	-7.53	-3.23	-2.83
m in kg/h	64566	64566	187143	113755	637748
T_{in} in °C	30.7	578.2	64.9	53.3	33.6
T_{out} in °C	140.0	160.0	30.0	30.0	30.0
p in bar	1	1	1	1	1
$phase_{in}$	gas/liquid	gas	liquid	liquid	liquid
$phase_{out}$	gas	gas	liquid	liquid	liquid

Table S13 – Operation conditions of the absorber column used for the FA(aq.) production based on MeOH and air. Numbering is presented in Figure S13.

	CO-1
Heat demand in MW	0.00
Cooling demand in MW	0.00
m_{Feed} in kg/h	64566
p in bar	1
T_{Dist} in °C	33.5
D:F in g/g	0.72
T_{Bott} in °C	64.9
number of stages	4
reflux:distillate in g/g	-

Table S14 – Operation conditions of the reactor used for the FA(aq.) production based on MeOH and air. Numbering is presented in Figure S13.

	R-FA
Cooling demand in MW	0.00
m_{Feed} in kg/h	64566
T_{in} in °C	140
T_{out} in °C	578
p in bar	1
Reactor type	fixed bed reactor
Heat management	adiabatic
$m_{Catalyst}$ in kg	2604
GHSV in h^{-1}	15000

Table S15 – Operation conditions of the compressor used for the FA(aq.) production based on MeOH and air. Numbering is presented in Figure S13.

	PC-1
Power in MW	1.04
Cooling demand in MW	0.00
m_{Feed} in kg/h	47287
p_{in} in bar	1.0
p_{out} in bar	1.8
T_{in} in °C	33.5
T_{out} in °C	100.3
$T_{intercooling}$ in °C	-
number of stages	1

4.2.3. FA concentration

Figure S14 illustrates a simplified process flow diagram of the FA concentration based on FA(aq.) solution. Furthermore, it presents the stream numbering for the stream compositions and conditions listed in Table S16.

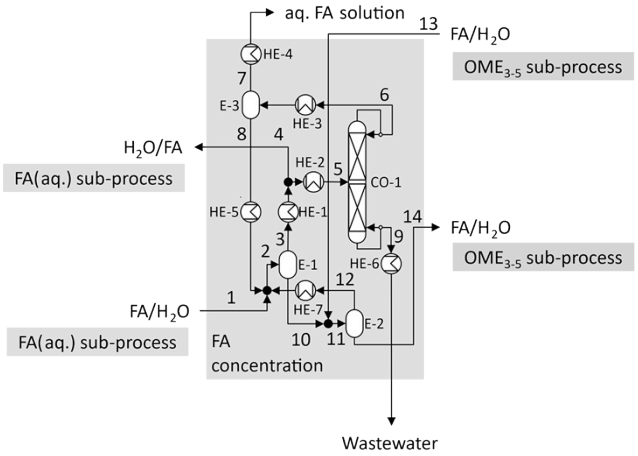

Figure S14 – Simplified process diagram of the FA concentration based on FA(aq.) solution. CO, distillation column; E, evaporator; HE, heat exchanger.

Table S16 – Stream table for the FA concentration based on FA(aq.) solution. The stream numbering is presented in Figure S13. The concentrations are presented in mass fractions.

	1	2	3	4	5	6	7	8	9	10	11	12	13	14
T in °C	64.9	76.1	76.1	40.0	149.8	120.1	118.3	118.3	155.5	76.1	88.5	88.5	117.4	88.5
p in bar	1.0	0.4	0.4	1.3	5.5	5.5	1.0	1.0	5.5	0.4	0.5	0.5	1.0	0.5
m in kg/h	18508	44273	14754	1231	13522	5652	2203	3449	7870	29520	45273	22316	15753	22957
FA	0.502	0.595	0.184	0.184	0.184	0.441	0.142	0.632	0.000	0.800	0.775	0.666	0.727	0.880
H_2O	0.491	0.399	0.796	0.796	0.796	0.510	0.778	0.340	1.000	0.200	0.224	0.331	0.268	0.120
MeOH	0.007	0.007	0.020	0.020	0.020	0.048	0.080	0.028	0.000	0.000	0.002	0.003	0.005	0.000

Table S17 to Table S19 present the operation conditions of the main process units of the FA concentration sub-process including heat exchangers, a distillation column and evaporators. Note that the operation conditions of the evaporators are different in practice with lower operation pressure and higher operation temperature. However, the applied model is not suitable to accurately describe the behavior inside the evaporators. Therefore, ideal separator unit operations were used to meet the mass balance and the operation conditions were adjusted to meet the phase of the streams and the heat demand. A detailed description of an advanced model for the simulation of the evaporators was published by Tönges et al.[44].

Table S17 – Operation conditions of the heat exchangers used for the FA concentration based on FA(aq.) solution. Numbering is presented in Figure S14.

	HE-1	HE-2	HE-3	HE-4	HE-5	HE-6	HE-7
Heat/cooling demand in MW	-9.92	1.63	1.12	-1.36	-0.08	-1.37	-8.92
m in kg/h	14754	13522	5652	2203	3449	7870	22316
T_{in} in °C	76.1	40.0	100.7	118.3	118.3	155.5	88.5
T_{out} in °C	40.0	149.8	118.3	30.0	90.0	30.0	86.2
p in bar	0.4	5.5	1.0	1.0	1.0	5.5	0.5
$phase_{in}$	gas	liquid	gas/liquid	gas	liquid	liquid	gas
$phase_{out}$	liquid	gas/liquid	gas/liquid	liquid	liquid	liquid	liquid

Table S18 – Operation conditions of the distillation column used for the FA concentration based on FA(aq.) solution. Numbering is presented in Figure S14.

	CO-1
Heat demand in MW	7.26
Cooling demand in MW	-7.10
m_{Feed} in kg/h	13522
p in bar	5.5
T_{Dist} in °C	120.1
D:F in g/g	0.42
T_{Bott} in °C	155.5
number of stages	32
reflux:distillate in g/g	1.2

Table S19 – Operation conditions of the evaporators used for the FA concentration based on FA(aq.) solution. Numbering is presented in Figure S14.

	E-1	E-2	E-3
Heat demand in MW	9.31	8.89	0.00
m_{Feed} in kg/h	44273	45273	5652
p in bar	0.4	0.5	1
T in °C	76.1	88.5	118.3

4.2.4. OME_{3-5} sub-process

Figure S15 illustrates a simplified process flow diagram of the OME_{3-5} sub-process based on MeOH and concentrated FA(aq.) solution. Furthermore, it presents the stream numbering for the stream compositions and conditions listed in Table S20.

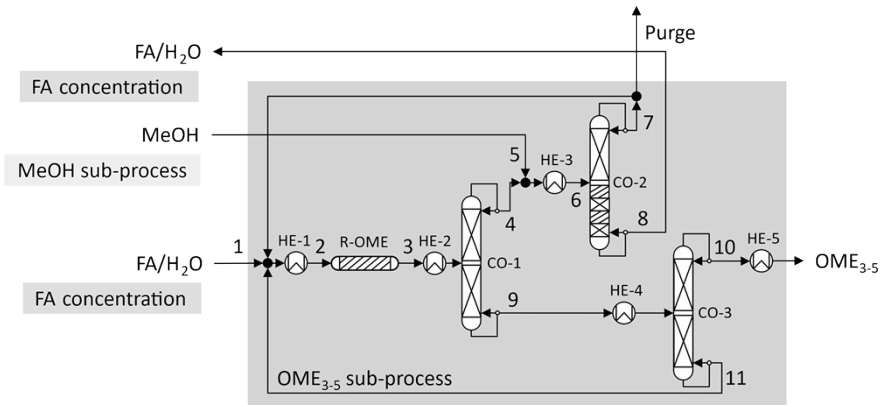

Figure S15 – Simplified process diagram for the production of OME_{3-5} from MeOH and concentrated FA(aq.) solution. CO, distillation column; HE, heat exchanger; R, reactor.

Table S20 – Stream table for the production of OME_{3-5} from MeOH and concentrated FA(aq.) solution. The stream numbering is presented in Figure S15. The concentrations are presented in mass fractions.

	1	2	3	4	5	6	7	8	9	10	11
T in °C	90.4	90.0	90.0	81.5	81.0	69.5	41.5	117.4	200.5	86.6	194.9
p in bar	10.3	10.0	10.1	1.8	1.8	1.0	1.0	1.0	1.8	0.1	0.1
m in kg/h	22957	66666	66666	51796	5288	57083	41330	15753	14871	12490	2380
FA	0.880	0.303	0.186	0.239	0.000	0.217	0.000	0.727	0.000	0.000	0.000
H_2O	0.120	0.042	0.022	0.028	0.000	0.026	0.002	0.268	0.000	0.000	0.000
MeOH	0.000	0.028	0.100	0.129	1.000	0.210	0.045	0.005	0.000	0.000	0.000
OME_1	0.000	0.591	0.276	0.356	0.000	0.323	0.953	0.000	0.000	0.000	0.000
OME_2	0.000	0.000	0.179	0.230	0.000	0.209	0.000	0.000	0.000	0.000	0.000
OME_3	0.000	0.000	0.107	0.017	0.000	0.015	0.000	0.000	0.419	0.499	0.000
OME_4	0.000	0.000	0.061	0.000	0.000	0.000	0.000	0.000	0.271	0.323	0.000
OME_5	0.000	0.000	0.033	0.000	0.000	0.000	0.000	0.000	0.149	0.177	0.000
OME_6	0.000	0.018	0.018	0.000	0.000	0.000	0.000	0.000	0.080	0.000	0.496
OME_7	0.000	0.009	0.009	0.000	0.000	0.000	0.000	0.000	0.042	0.000	0.262
OME_8	0.000	0.005	0.005	0.000	0.000	0.000	0.000	0.000	0.022	0.000	0.136
OME_9	0.000	0.002	0.002	0.000	0.000	0.000	0.000	0.000	0.011	0.000	0.070
OME_{10}	0.000	0.001	0.001	0.000	0.000	0.000	0.000	0.000	0.006	0.000	0.036

Table S21 to Table S23 present the operation conditions of the main process units of the OME_{3-5} sub-process including heat exchangers, distillation columns and a reactor. Note that the WHSV of the OME reactor is overestimated and much lower in practice. The complexity is described in the manuskript.

Table S21 – Operation conditions of the heat exchangers used for the production of OME_{3-5} from MeOH and concentrated FA(aq.) solution. Numbering is presented in Figure S15.

	HE-1	HE-2	HE-3	HE-4	HE-5
Heat/cooling demand in MW	1.52	5.01	0.12	0.39	-0.32
m in kg/h	66666	66666	57083	14871	12490
T_{in} in °C	58.6	90.0	76.4	120.2	86.6
T_{out} in °C	90.0	130.0	69.5	130.0	30.0
p in bar	10	2	1	0.1	1.0
$phase_{in}$	liquid	liquid	gas/liquid	gas/liquid	liquid
$phase_{out}$	liquid	gas/liquid	gas/liquid	gas/liquid	liquid

Table S22 – Operation conditions of the distillation columns used for the production of OME_{3-5} from MeOH and concentrated FA(aq.) solution. Numbering is presented in Figure S15.

	CO-1	CO-2	CO-3
Heat demand in MW	12.69	4.47	0.47
Cooling demand in MW	-17.17	-7.90	-1.67
m_{Feed} in kg/h	66666	57083	14871
p in bar	1.8	1	0.07
T_{Dist} in °C	81.5	41.5	86.6
D:F in g/g	0.78	0.72	0.84
T_{Bott} in °C	200.5	117.4	194.9
number of stages	56	40	30
reflux:distillate in g/g	0.5	0.7	0.3

Table S23 – Operation conditions of the reactor used for the production of OME_{3-5} from MeOH and concentrated FA(aq.) solution. Numbering is presented in Figure S15.

	R-OME
Heat demand in MW	0.49
m_{Feed} in kg/h	66666
T_{in} in °C	90
T_{out} in °C	90
p in bar	10
Reactor type	fixed bed reactor
Heat management	isothermal
$m_{Catalyst}$ in kg	952
WHSV in h^{-1}	70

4.2.5. Combustion

Figure S16 illustrates a simplified process flow diagram for the combustion of the purge streams. Furthermore, it presents the stream numbering for the stream compositions and conditions listed in Table S24.

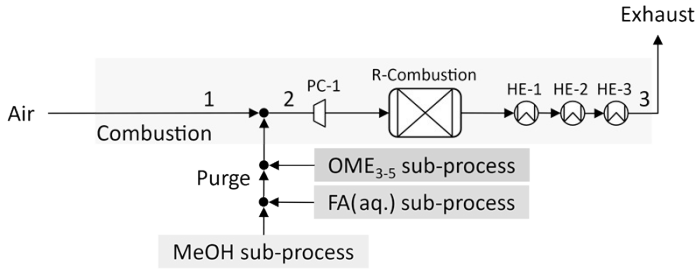

Figure S16 – Simplified process diagram for the combustion of the purge streams. HE, heat exchanger; PC, compressor; R, reactor.

Table S24 – Stream table for the combustion of the purge streams. The stream numbering is presented in Figure S16. The concentrations are presented in mass fractions.

	1	2	3
T in °C	25.0	54.6	98.5
p in bar	1.0	1.0	1.0
m in kg/h	34730	54838	54838
FA	0.000	0.001	0.000
H_2O	0.000	0.012	0.063
MeOH	0.000	0.001	0.000
H_2	0.000	0.005	0.000
CO_2	0.000	0.031	0.036
CO	0.000	0.002	0.000
N_2	0.742	0.753	0.753
O_2	0.258	0.195	0.147

Table S25 to Table S27 present the operation conditions of the main process units for the combustion of the purge streams including heat exchangers, a combustion chamber and a compressor.

Table S25 – Operation conditions of the heat exchangers used for the combustion of the purge streams. Numbering is presented in Figure S16.

	HE-1	HE-2	HE-3
Heat/cooling demand in MW	-9.68	-1.16	-1.32
m in kg/h	54838	54838	54838
T_{in} in °C	772.9	230.0	160.0
T_{out} in °C	230.0	160.0	98.5
p in bar	2.0	1.7	1.3
$phase_{in}$	gas	gas	gas
$phase_{out}$	gas	gas	gas

Table S26 – Operation conditions of the reactor used for the combustion of the purge streams. Numbering is presented in Figure S16.

	R-Combustion
Heat demand in MW	0.00
m_{Feed} in kg/h	54838
T_{in} in °C	151
T_{out} in °C	773
p in bar	2
Reactor type	Combustion chamber
Heat management	steam generation

Table S27 – Operation conditions of the compressor used for the combustion of the purge streams. Numbering is presented in Figure S16.

	PC-1
Power in MW	1.61
Cooling demand in MW	0.00
m_{Feed} in kg/h	54838
p_{in} in bar	1.0
p_{out} in bar	2.1
T_{in} in °C	54.6
T_{out} in °C	150.7
$T_{intercooling}$ in °C	-
number of stages	1

4.3. Comparison to alternative OME_{3-5} production processes

The key assumptions for the overall energy efficiency of various OME_{3-5} production processes including the production of H_2 via H_2O electrolysis and various CO_2 capture techniques are summarized in Table S28. The assumptions were considered from Held et al.[7].

Table S28 – Energy demand for H_2O electrolysis and various CO_2 capture techniques[7]. CPS, CO_2 from point sources; PCC, postcombustion capture; DAC, direct air capture.

	H_2O electrolysis	CPS	PCC	DAC
Electricity demand in MJ/kg product	200.2	0.0	0.0	0.9
Heat demand in MJ/kg product	0.0	0.0	3.33	6.3

References

1. H. Schelling, E. Ströfer, R. Pinkos, A. Haunert, G.-D. Tebben, H. Hasse and S. Blagov, *Method for producing Polyoxymethylene Dimethyl Ethers*, BASF Aktiengesellschaft(US 20070260094A1), 2007.
2. J. Burger, *A novel process for the production of diesel fuel additives by hierarchical design*, Ph.D. Thesis, University of Kaiserslautern, Kaiserslautern, 2012.
3. J. Burger, M. Siegert, E. Ströfer and H. Hasse, *Fuel*, 2010, **89**, 3315.
4. F. Mantei, S. Kopp, A. Holfelder, E. Flad, D. Kloeters, M. Kraume and O. Salem, *React. Chem. Eng.*, 2023. 10.1039/D2RE00508E.
5. L. Lautenschütz, *Neue Erkenntnisse in der Syntheseoptimierung oligomerer Oxymethylendimethylether aus Dimethoxymethan und Trioxan*, Ph.D. Thesis, Heidelberg, 2015.
6. T. Grützner, H. Hasse, N. Lang, M. Siegert and E. Ströfer, *Chemical Engineering Science*, 2007, **62**, 5613.
7. M. Held, Y. Tönges, D. Pélerin, M. Härtl, G. Wachtmeister and J. Burger, *Energy Environ. Sci.*, 2019, **12**, 1019.
8. J. Burre, D. Bongartz and A. Mitsos, *Ind. Eng. Chem. Res.*, 2019, **58**, 5567.
9. C. F. Breitkreuz, M. Dyga, E. Forte, F. Jirasek, J. de Bont, J. Wery, T. Grützner, J. Burger and H. Hasse, *Chemical Engineering and Processing - Process Intensification*, 2021, 108710.
10. Projects. https://www.carbonrecycling.is/projects, (last accessed June 2022).
11. A. W. Franz, H. Kronemayer, D. Pfeiffer, R. D. Pilz, G. Reuss, W. Disteldorf, A. O. Gamer and A. Hilt, eds., *Ullmann's Encyclopedia of Industrial Chemistry: Formaldehyde*, Wiley-VCH Verlag GmbH & Co. KG, Weinheim, 2016.
12. F. Mantei, R. E. Ali, C. Baensch, S. Voelker, P. Haltenort, J. Burger, R.-U. Dietrich, N. von der Assen, A. Schaadt, J. Sauer and O. Salem, *Sustainable Energy Fuels*, 2022, **6**, 528.
13. E. Ströfer, H. Schelling, H. Hasse and S. Blagov, *METHOD FOR THE PRODUCTION OF POLYOXYMETHYLENE DIALKYLETHERS FROM TROXAN AND DIALKYLETHERS: US*(US007999140B2), 2011.
14. C. F. Breitkreuz, N. Schmitz, E. Ströfer, J. Burger and H. Hasse, *Chemie Ingenieur Technik*, 2018, **90**, 1489.
15. S. Schemme, J. L. Breuer, M. Köller, S. Meschede, F. Walman, R. C. Samsun, R. Peters and D. Stolten, *International Journal of Hydrogen Energy*, 2020, **45**, 5395.
16. P. Haltenort, K. Hackbarth, D. Oestreich, L. Lautenschütz, U. Arnold and J. Sauer, *Catalysis Communications*, 2018, **109**, 80.
17. P. Haltenort, L. Lautenschütz, U. Arnold and J. Sauer, *Top Catal*, 2019, **62**, 551.
18. M. Drexler, P. Haltenort, U. Arnold and J. Sauer, *Chem. Ing. Tech.*, 2022, **94**, 256.
19. M. Drexler, P. Haltenort, U. Arnold, J. Sauer, S. A. Karakoulia and K. S. Triantafyllidis, *Catalysis Today*, 2022. 10.1016/j.cattod.2022.07.015.
20. C. F. Breitkreuz, N. Hevert, N. Schmitz, J. Burger and H. Hasse, *Ind. Eng. Chem. Res.*, 2022, **61**, 7810.
21. A. T. Sundberg, P. Uusi-Kyyny, M. Pakkanen and V. Alopaeus, *J. Chem. Eng. Data*, 2011, **56**, 2634.
22. S. Lee, J. Cho and Y.-C. Kim, *Fluid Phase Equilibria*, 2015, **397**, 95.
23. S. Adelung, J. Artz, R. U. Dietrich, J. Hildebrand, L. López, Y. P. Rahmat, N. van der Assen and …, *NAMOSYN Nachhaltige Mobilität durch synthetische Kraftstoffe: Abschlussbericht*, 2022.
24. J. Sauer and G. Emig, *Chem. Eng. Technol.*, 1995, **18**, 284.
25. S. Su, P. Zaza and A. Renken, *Chem. Eng. Technol.*, 1994, **17**, 34.
26. Y. Liu, Y. Wang and W. Cai, *Trans. Tianjin Univ.*, 2018, **39**, 918.
27. A. Peter, G. Stebens, J. F. Baumgärtner, E. Jacob, F. K. Mantei, M. Ouda and I. Krossing, *ChemCatChem*, 2020, **12**, 2416.
28. Z. Ye and J. Xiang, *Formaldehyde absorption process device and method in polyoxymethylene dimethylether synthesis: WO*(2016/180085 A1), 2016. https://patents.google.com/patent/WO2016180085A1/en?oq=WO+2016%2f180085+A1.
29. N. Schmitz, E. Ströfer, J. Burger and H. Hasse, *Industrial & Engineering Chemistry Research*, 2017, **56**, 11519.
30. J. Burger, N. Schmitz, H. Hasse and E. Ströfer, *Process for preparing Polyoxymethylene Dimethyl Ethers from Formaldehyde and Methanol in aqueous solutions*(US 2018/0134642 A1), 2018.
31. N. Schmitz, J. Burger and H. Hasse, *Industrial & Engineering Chemistry Research*, 2015, **54**, 12553.
32. N. Schmitz, F. Homberg, J. Berje, J. Burger and H. Hasse, *Industrial & Engineering Chemistry Research*, 2015, **54**, 6409.

33. A. Ferre, J. Voggenreiter, Y. Tönges and J. Burger, *MTZ Motortech Z*, 2021, **82**, 28.
34. J. Voggenreiter, A. Ferre and J. Burger, *Ind. Eng. Chem. Res.*, 2022. 10.1021/acs.iecr.2c01468.
35. K. Hackbarth, P. Haltenort, U. Arnold and J. Sauer, *Chem. Ing. Tech*, 2018, **90**, 1.
36. R. Palkovits, C. H. Gierlich and I. Delidovich, *Verfahren zur Trennung von Oxymethylenethern: EP*(EP 3 514 134 A1), 2019.
37. C. H. Gierlich, *Herstellung von Oxymethylenethern anhand von alternativen Reaktionskonzepten*, Ph.D. Thesis, Aachen, 2021.
38. G. P. Hagen and M. J. Spangler, *PREPARATION OF POLYOXYMETHYLENE DIMETHYL ETHERS BY CATALYTIC CONVERSION OF FORMALDEHYDE FORMED BY OXIDATION OF DIMETHYL ETHER: US*(US 6392102 B1), 2002.
39. J.-O. Drunsel, *Entwicklung von Verfahren zur Herstellung von Methylal und Ethylal*, Ph.D. Thesis, Scientific Report Series, Kaiserslautern, 2012.
40. T. Qiang, W. Jinfu, W. Tiefeng and Z. Yanyan, *METHOD FOR PREPARING DMM3-5 FROM HYPERCOAGULABLE POLYOXYMETHYLENE DIMETHYL ETHER COMPONENT DMM6+ AND DIMETHOXYMETHANE DMM: CN*(CN105152882 A), 2017.
41. Xiangjun Li, Huaiyuan Tian, Wujie Zhang and Dianhua Liu, *International Journal of Chemical and Molecular Engineering*, 2018, 536.
42. D. Oestreich, L. Lautenschütz, U. Arnold and J. Sauer, *Fuel*, 2018, **214**, 39.
43. N. Schmitz, C. F. Breitkreuz, E. Ströfer, J. Burger and H. Hasse, *Journal of Membrane Science*, 2018, **564**, 806.
44. Y. Tönges and J. Burger, *Chemical Engineering Research and Design*, 2022. 10.1016/j.cherd.2022.11.022.